

Màster oficial en

***Modelització Computacional Atomística i Multiescala
en Física, Química i Bioquímica***

Treball Final de Màster

Moviment col·lectiu, vols de Lévy i fenòmens de sincronització en bancs de peixos

Movimiento colectivo, vuelos de Lévy y fenómenos de sincronización en bancos de peces

Collective motion, Levy flights and synchronization phenomena in schooling fish

Jordi Torrents Monegal

Setembre del 2020

Aquesta obra esta subjecta a la llicència de:
Reconeixement-NoComercial-SenseObraDerivada



<http://creativecommons.org/licenses/by-nc-nd/3.0/es/>

Simplificar per anar més enllà.

Aquest treball pot tenir només un responsable, però mai tindrà només un autor. Totes les persones que, d'una forma o altra, han estat presents en l'esdevenir d'aquest projecte estaran sempre lligades en l'autoria no oficial d'aquest. És per això que vull agrair a la meva família, amics i especialment a la Irina pel constant suport i amor.

Tampoc no es pot entendre un estudi científic sense la comunitat, sense la col·laboració i l'ajuda. Vull agrair a M. Carmen Miguel la seva entrega, dedicació i generositat. De igual manera al meu grup de treball per proporcionar dades i estudis en pro del coneixement i la descoberta. He tingut la gran sort de poder desenvolupar aquest projecte en el sí d'una beca amb l'Institut de Sistemes Complexos de la Universitat de Barcelona (UBICS) que, tot i fer el treball confinat a casa, ha estat de molta ajuda i suport.

Finalment vull agrair a tota la comunitat acadèmica i totes aquelles persones que han seguit endavant tot i les dificultats produïdes per la CODIV-19 i tot el que ha suposat en aquest curs acadèmic tan difícil. A aquestes, tot el meu respecte i admiració.

Títol: Moviment col·lectiu, vols de Lévy i fenòmens de sincronització en bancs de peixos

Estudiant: Jordi Torrents Monegal

Data: Setembre 2020

Director/s: Dra. M. Carmen Miguel

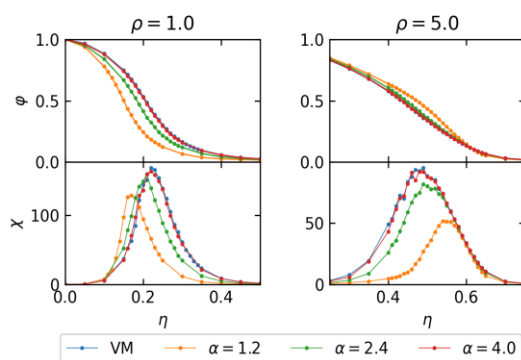
Departament de Física Fonamental

S'anomena moviment col·lectiu a l'autoorganització entre individus en moviment que arriben a un desplaçament grupal i coherent només a través d'interaccions locals deixant de banda qualsevol influència externa o central. Aquest tipus de dinàmica és present en la conducta d'una gran varietat de grups d'éssers vius com ara colònies bacterianes, insectes, ramats d'aus, bancs de peixos i humans en multituds. Es creu que aquest comportament és essencial per a la supervivència de les espècies, els membres de les quals es comporten completament diferent de la manera en què ho farien pel seu compte.

Els mecanismes que regeixen totes aquestes conductes semblen tenir fonaments universals i un interès creixent ha aparegut en aquest camp a cavall de diverses disciplines científiques.

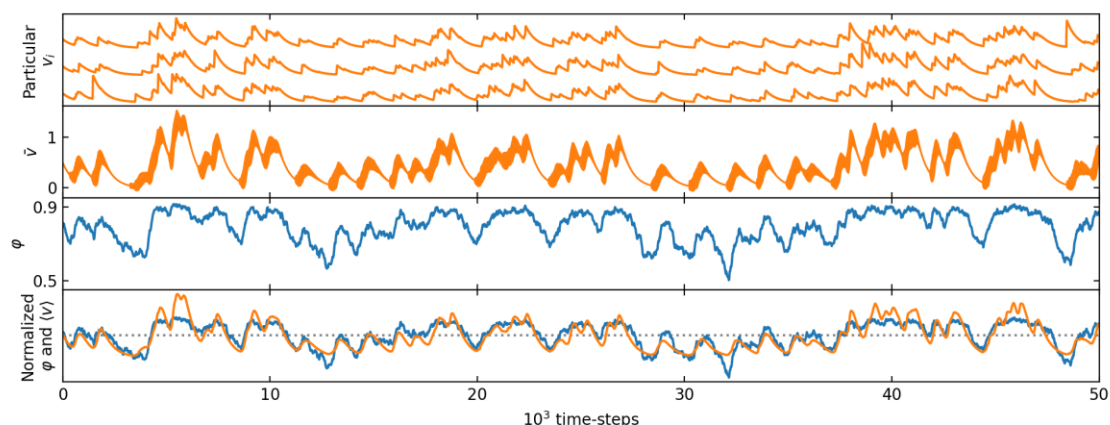
En aquest projecte, s'ha estudiat el fenomen col·lectiu utilitzant el model de Vicsek com a primera aproximació per estudiar les estructures dinàmiques en peixos i la seva ordenació polar. Aquest model aconsegueix imitar algunes conductes bàsiques dels animals a través de, només, una simple regla d'alineació. Aquí es presenta un breu estudi sobre això.

Però les observacions experimentals del nostre grup de recerca i altres dades publicades desafien el model més senzill i ens inspiren a proposar dos nous models per apropar les simulacions d'estil Vicsek al moviment col·lectiu real.



Comparativa de la polarització global ϕ i la seva susceptibilitat χ pel model Lévy (amb diferents paràmetres de la llei de potències α) i el clàssic model de Vicsek per dos valors de la densitat.

Per una banda, la presència de comportaments de Lévy en grups de peixos ens porta a la idea d'afegir un comportament de Lévy amb vols en llei de potència a les partícules del model clàssic. Això, en sistemes de baixa densitat, és perjudicial pel que fa a la polarització, perquè els vols en llei de potència trenquen els resistents cúmuls de partícules d'alta densitat (típics del model de Vicsek) i això fa disminuir l'ordre global. Però a densitats prou altes, el comportament de Lévy aporta una major connectivitat social i, per tant, una millora en l'ordre i el rendiment.



Evolució temporal de: **Primer gràfic**, la velocitat de tres partícules aleatòries. **Segona gràfica**, la velocitat mitjana de totes les partícules amb la seva desviació estàndard representada en el gruix de la línia. **Tercera gràfica**, polarització del grup i, **quarta gràfica**, una superposició normalitzada de la velocitat mitjana (línia taronja) amb la polarització (línia blava).

Per altra banda, s'ha creat un model més sofisticat amb dinàmica tipus *burst-and-coast*, amb *bursts* com a processos aleatoris de *Poisson* i imitació de velocitats asimètrica per modelar les oscil·lacions coherents observades en la velocitat mitjana del grup així com també la provada correlació positiva entre la velocitat mitjana del grup i la seva polarització en grups de peixos. Els nostres resultats concorden qualitativament amb les nostres observacions en el grup de recerca, així com amb la literatura publicada existent.

Título: Movimiento colectivo, vuelos de Lévy y fenómenos de sincronización en bancos de peces

Estudiante: Jordi Torrents Monegal

Fecha: Setiembre 2020

Director/es: Dra. M. Carmen Miguel

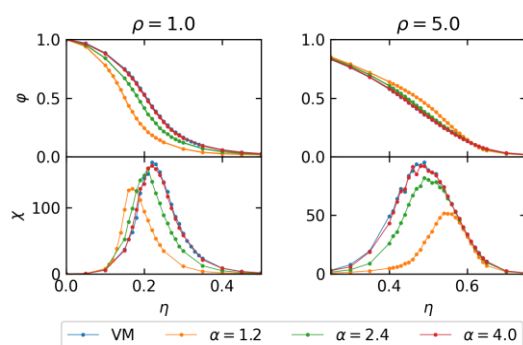
Departament de Física Fonamental

Se denomina movimiento colectivo a la autoorganización entre individuos en movimiento que llegan a un desplazamiento grupal y coherente sólo a través de interacciones locales dejando de lado cualquier influencia externa o central. Este tipo de dinámica está presente en la conducta de una gran variedad de grupos de seres vivos como colonias bacterianas, insectos, rebaños de aves, bancos de peces o hasta humanos en multitudes. Se cree que este comportamiento es esencial para la supervivencia de las especies, los miembros de las cuales se comportan completamente diferente de la manera en que lo harían por su cuenta.

Los mecanismos que rigen todas estas conductas parecen tener unos fundamentos universales y un interés creciente ha aparecido en este campo en la frontera de varias disciplinas científicas.

En este proyecto, se ha estudiado el fenómeno colectivo utilizando el modelo de Vicsek como primera aproximación para estudiar las estructuras dinámicas en peces y su ordenación polar. Este modelo consigue imitar algunas conductas básicas de los animales a través de, sólo, una simple regla de alineación. Aquí se presenta un breve estudio sobre ello.

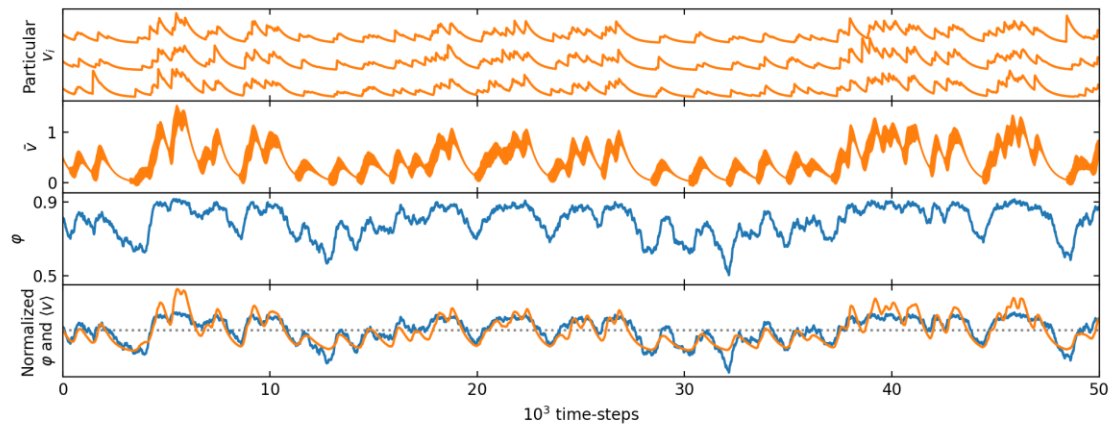
Pero las observaciones experimentales de nuestro grupo de investigación y otros datos publicados desafían el modelo más sencillo y nos inspiran a proponer dos nuevos modelos para acercar las simulaciones de estilo Vicsek al movimiento colectivo real observado.



Comparación de la polarización global ϕ y su susceptibilidad χ para el modelo de Lévy (con diferentes valores de ley de potencias α) y el modelo clásico de Vicsek para dos valores de densidad.

Por un lado, la presencia de comportamientos de Lévy en grupos de peces nos lleva a la idea de añadir un comportamiento de Lévy con vuelos en ley de potencia a las partículas del modelo clásico. Esto, en sistemas de baja densidad, es perjudicial en cuanto a la polarización, porque los vuelos en ley de potencia rompen los resistentes cúmulos de partículas de alta densidad (típicos del modelo de Vicsek) y esto hace disminuir el orden global. Pero a densidades suficientemente altas donde los clústers no se pueden deshacer, el

comportamiento de Lévy aporta una mayor conectividad social y, por tanto, una mejora en el orden y el rendimiento.



Evolución temporal de: **Primero gráfico**, la velocidad de tres partículas aleatorias. **Segunda gráfica**, la velocidad media de todas las partículas con su desviación estándar representada en el grosor de la línea. **Tercera gráfica**, polarización del grupo y, **cuarta gráfica**, una superposición normalizada de la velocidad media (línea naranja) con la polarización (línea azul).

Por otra parte, se ha creado un modelo más sofisticado con dinámica tipo burst-and-coast, con bursts aleatorios como procesos de Poisson e imitación asimétrica de velocidades para modelar las oscilaciones coherentes observadas en la velocidad media del grupo y, también, la evidenciada correlación positiva entre la velocidad media del grupo y su polarización en bancos de peces. Nuestros resultados concuerdan cualitativamente con nuestras observaciones en el grupo de investigación, así como con la literatura publicada existente.

Title: **Collective motion, Levy flights and synchronization phenomena in schooling fish**

Student: Jordi Torrents Monegal

Date: September 2020

Supervisor/s: Dra. M. Carmen Miguel

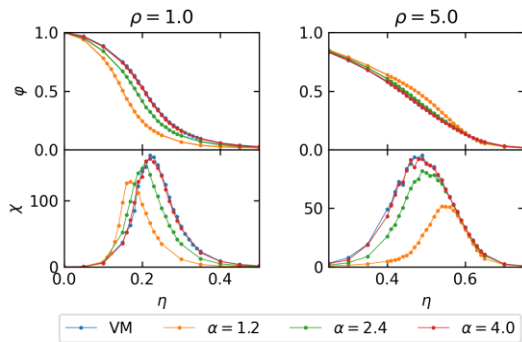
Departament de Física Fonamental

Collective motion is said to be the self-organization between moving individuals reaching a spontaneous emergence of coherent group displacement and order with just local interactions neglecting any external or central influence. This motion is found in a wide variety of animals and microbiological groups conduct such as bacterial colonies, insects, bird flocks, fish schools and human crowds. This behaviour is thought to be essential for the species survival, of which individuals behave entirely differently from the way it would behave on its own.

The underlying mechanisms all these conducts seem to have quite universal basis and an increasing interest has appeared in this emerging field on the borderline of several scientific disciplines.

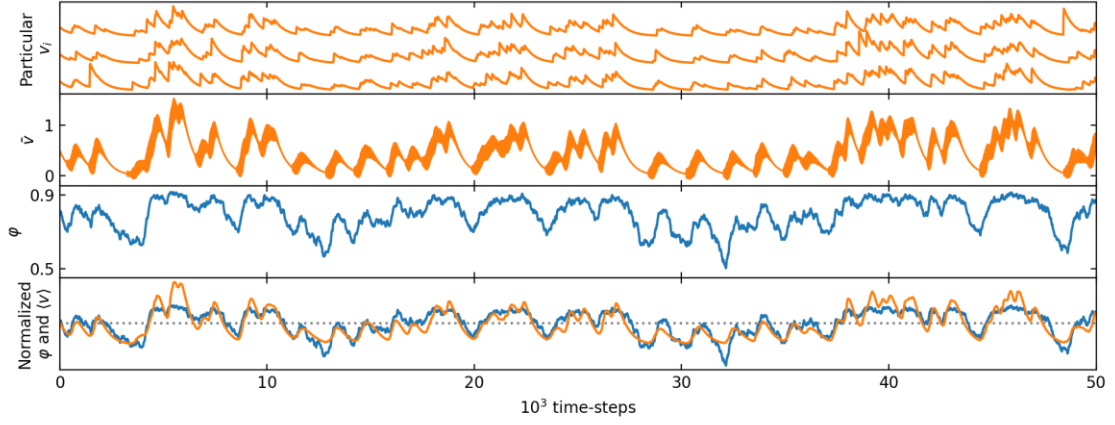
In this project, collective motion has been discussed using Vicsek model as the main approach to study dynamical structures in fish schooling and their polar ordering. This model mimics some basic animal conduct with just a simple alignment rule. A brief study is done about that model.

But experimental observations within our research group and other published data challenges the simplest model and inspire us to propose two new Vicsek-like models to get closer to experimental observations.



Comparison of global polarization ϕ and its susceptibility χ for the Lévy model (with different power-law values α) and the classic Vicsek model for two density values.

On one hand, the presence of Lévy behaviour on fish groups brings us the idea to add a Lévy behaviour with power-law flights to the particles in the classic model. This, at low system densities, is found to be prejudicial in terms of polarization because power-law flights break the high density and resistant particle clusters (typical of the Vicsek model) and, thus, the global order decreases. But at higher enough densities, where clusters cannot break up, Lévy behaviour brings a higher social connectivity and, hence, a better performance in terms of group polarization.



Temporal evolution of: First plot, the speed of three random particles. Second plot, the average speed of all particles with its standard deviation represented in the line width. Third plot, group polarization and, Fourth plot, a normalized superposition of the mean speed (orange line) and polarization (blue line) four our second model.

On the other hand, a more sophisticated model with burst-and-coast dynamics, Poisson distributed random bursts and speed imitation has been used to model the observed coherent oscillations on fish schools' swimming speed and, at the same time, to corroborate the proven positive correlation between the average group speed and its polarization in a rather satisfactory manner. Our results agree qualitatively with our observations in the research group as well as the existing published literature.

Prèviament a aquest treball, el grup de recerca ja havia fet les observacions en peixos i les primeres dades d'aquestes ja es coneixien. A més, el grup, amb J. Múgica, R. Pastor-Satorras i C. Miguel, ja tenia a mig fer el *preprint* sobre el model de Vicsek i la sincronització velocitat-polarització. Faig constar que la meua contribució en aquest treball ha consistit en (en ordre temporal):

- La recerca bibliogràfica, amb l'ajuda de la tutora Carmen Miguel, de dades experimentals i treballs fets amb l'objectiu d'estudiar i modelitzar comportaments col·lectius i, en específic, en grups de peixos.
- El desenvolupament del programa en Fortran del model de Vicsek i diferents models ja existents des de zero amb la deguda optimització de codi utilitzant els coneixements adquirits en el màster.
- Una primera etapa de "creativitat" on, amb tot l'exposat, s'han proposat fins a 14 models diferents (a l'estil Vicsek o no) fruit de llargues reflexions autor-tutora. S'han provat interaccions d'orientació amb pes, interaccions de velocitat, passos de temps desiguals entre partícules, algoritmes de Gillespie per fer simulacions estocàstiques, models realistes altament parametritzats...
- La posterior computació de tots aquests models ampliant el codi desenvolupat anteriorment en un sol programa molt versàtil.
- Comparació i discussió de resultats dels tots els models relacionant-los entre ells i amb les dades experimentals amb l'ajuda de la tutora.
- Una segona etapa de "creativitat" on, amb el coneixement de la primera etapa i les noves dades observacionals, s'han proposat (amb l'ajuda de la tutora) 2 nous models més sofisticats i profunds els quals s'han programat.
- Última comparativa de resultats i tria del material vàlid per presentar al treball (un model de cada etapa) amb el posterior anàlisi exhaustiu i redactat del treball.

FORMATTED REPORT

Collective motion, Lévy flights and synchronization phenomena in schooling fish

Author: Jordi Torrents Monegal | **Advisor:** M. Carmen Miguel

*Facultat de Física i Química, UNIVERSITAT DE BARCELONA, Diagonal 645, 08028 Barcelona, Spain**

(Dated: September 2020)

Abstract. Collective motion has been discussed using the Vicsek model as the main approach for fish flocking and polar ordering. Starting from this simple model, and inspired by experimental observations within our research group and other published data, we propose two different models to get the Vicsek model closer to the real collective motion observed in experiments. On one hand, the presence of Lévy behaviour on fish groups brings us the idea to add a Lévy behaviour with power-law flights to particles in the classic model. Lévy flights, at high enough densities, bring a higher social connectivity and, hence, a better performance in terms of group polarization. On the other hand, a more sophisticated model with burst-and-coast dynamics, Poisson distributed random bursts and speed imitation has been used to model the observed coherent oscillations on fish schools' swimming speed and, at the same time, to corroborate the proven positive correlation between the average group speed and its polarization in a rather satisfactory manner. Both models are presented and discussed. The corresponding simulation codes are also explained and published.

I. INTRODUCTION

Several animal groups appear to behave as if they were a single organism and exhibit quite synchronized movements. Members of these groups self-organize with each other via local interactions with no external or central influence reaching a spontaneous emergence of coherent group displacement and order in the so-called collective motion. There, individual action is dominated by the influence of the “others”, the unit behaves entirely differently from the way it would behave on its own [1].

Collective motion is also found in many other active matter systems where alive particles move on its own, for example bacterial colonies, fish schools, bird flocks and human crowds. Under certain conditions, these systems can present a transition to an ordered state with this type of motion. The wide variety of systems presenting the same phenomena with similar characteristics indicate some universal underlying laws, i.e. the collective phenomena does not depend entirely on the nature of the system, its laws are transferable across different species and scenarios.

The interest in the study of these phenomena from a physical perspective has grown in the past years due to the building of very simple and general models which capture the universal essence of collective motion and still can be studied using the well known methodology of statistical physics, complexity and computational sciences.

The most celebrated model for collective motion was written in 1995 by T. Vicsek *et al.* [2] and is commonly known as the Vicsek Model (VM). The VM extracts a very simple and universal interaction rule that, we will see, is the foundation of a wide variety of models and studies. But, while the simplest VM explains the emergence of global order in animal groups as well as other dynamic and structural properties of real observations

(especially on fish flocking), it cannot reflect new evidences of real data found on experimental observations. The Vicsek model is thus not enough.

Scientists have started to observe real collective motion on animals, especially on fishes, with image processing and tracking. As new rigorous experimental studies are done in this field, more common patterns in fish group dynamics are being found and the simplest VM is no longer able to reproduce them. In addition to the existing published experimental data, in our research group, experimental observations of groups of black neon tetra (*Hyphessobrycon herbertaxelrodi*) swimming freely in an experimental tank have been done. All that experimental data indicates deeper and more complex mechanisms on fish behaviour that has been constructed by natural selection and, hence, they may present benefits for the species they belong to. So far, experimental pieces of knowledge indicate that:

- Fish present a Lévy-like behaviour within their group with super-diffusive dynamics [3].
- Fish individual speeds are not fixed in time [4], nor is the average group speed [5].
- There exists a positive correlation between the group mean speed and its polarization [5].

Willing to untangle the mechanisms that make possible the above-mentioned individual and collective features, but without losing universality and getting lost in peculiarities and highly parametrized models, we look for the relevant interactions and details that do have an implication on the global behaviour of fish groups. In this paper, first we are gonna present the classic VM and its interesting properties in order to, then, modify it and propose two new Vicsek-like models inspired in real observations. This will bring us a deeper understanding of collective motion in groups of fishes and its underlying ruling laws.

*Electronic address: jordi.torrentsm@gmail.com

II. THE VICSEK MODEL OF COLLECTIVE MOTION

In the VM, and the majority of models of this field, the nature of a living group member and all its internal physics and processes (energy consumption, internal movements, life expressions, logic, etc.) are modeled far away from a molecular dynamic style. All its nature is coarse-grained into a self-propelling particle (SPP) entity whom does not obey inertia Newton's law (no momenta conservation) but has its own laws [1].

VM (following its original description [2]) consists of having N SPPs in a simulation space (normally 2D) of size L with periodic boundary conditions (PBCs). Particles are defined by their position \mathbf{r}_i (where i indicates particle index) and an orientation angle θ_i . To integrate the system from time t to time $t + \Delta t$, VM proposes a local orientation alignment rule followed by a strength-defined stochastic angular noise. These rules are stated as

$$\left. \begin{aligned} \theta_i^{t+\Delta t} &= \langle \theta_j^t \rangle_{R_0} + \eta \xi_i^t \\ \mathbf{r}_i^{t+\Delta t} &= \mathbf{r}_i^t + \Delta x \mathbf{s}_i^{t+\Delta t} \end{aligned} \right\} \text{VM equations} \quad (1)$$

where ξ_i^t is a zero average, delta-correlated scalar noise

$$\langle \xi_i^t \rangle = 0 \quad \langle \xi_i^t \xi_j^k \rangle \sim \delta_{tk} \delta_{ij}$$

uniformly distributed in $[-\pi, \pi]$, η is the noise strength ranging from 0 to 1, $\mathbf{s}_i = (\cos \theta_i, \sin \theta_i)$ is the unitary orientation vector defined by θ_i , $\langle \theta_j^t \rangle_{R_0}$ represents the averaged direction of all particles j closer than R_0 from particle i at time t , and Δx is the particle's travelled distance in one time-step (in one *flight*), which is constant.

In this model time-steps are uniform and space-time units are set so that $\Delta t = R_0 = 1$. In the literature [2], the term Δx is usually written as $\Delta x = \Delta t v_0$ where v_0 represents a particle's speed. As the time-step is always set to $\Delta t = 1$, we have $\Delta x = v_0$ so choosing Δx is just a notation detail that will be useful in the future. Then, the four final control parameters in the VM are:

- the number of particles N ,
- the noise amplitude η ,
- the flight distance Δx , and
- the total density of particles $\rho = N/L^2$.

Following a statistical point of view, collective properties are the ones we are interested in. The main observable, which will be also an order parameter, is the polarization φ defined as

$$\varphi \equiv \frac{1}{N} \left| \sum_{i=1}^N \mathbf{s}_i \right| \quad (2)$$

which can go from 0 (fully disordered system) to 1 (fully ordered and polarized).

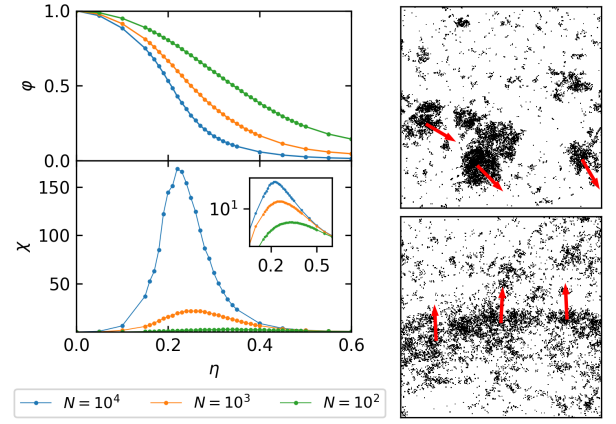


Figure 1: **Top left:** Polar order φ as a function of the noise amplitude η during 10^6 time-steps simulations, $\rho = 1.0$ and $\Delta x = 0.03$ for three different values of N , the number of particles in the simulation box. **Bottom left:** Susceptibility ($\chi \equiv N \cdot \sigma^2$) of φ for the same simulation as Top left with a log-log representation of the same data in the inset plot. **Top right:** Snapshot of the VM dynamics with $N = 10^4$, $\rho = 1.0$, $\eta = 0.2$ and $\Delta x = 0.03$ where typical Vicsek clusters mimicking flocking behaviour. Red arrows indicate the main direction of motion of the flock. **Bottom right:** Snapshot of the same dynamics as in Top right but with $\Delta x = 0.3$ (10 times bigger) presenting closed bands.

The VM presents a phase transition as a function of the noise amplitude η from a disordered phase with $\varphi \rightarrow 0$ for high η , where particles experience independent random walks, and a global ordered phase with $\varphi \rightarrow 1$ for low η where all particles have the same direction of movement (see Figure 1 top left and bottom left). In this ordered phase, an interesting flocking behaviour emerges without being explicitly imposed (see Figure 1 Top right) that, as we will see later, has a very important role on collective order. However, the nature of this phase transition is rather non-trivial and have stimulated hot discussions among several research groups in the past years.

In the original VM proposal [2], a continuous phase transition was observed with a statistically homogeneous density field (at large scale) in the frame moving at the global velocity. But, with higher system sizes and higher velocities, in [6] H. Chaté demonstrated a first order phase transition using the same VM laws. New structures were found for noise amplitudes lower but near the critical point with particles shaping *well-defined high-density and high-order propagating solitary structures* [6], in other words, closed bands across the system (Figure 1 Bottom right, as system size increase these bands grow up and become more evident, for our simulation with $N = 10^4$ the band is rather weak). These bands (there can be more than one if the system is large enough) cross the simulation box from side to side moving on the transverse direction. The formation of these very noise-resistant bands in the ordered phase, for η close to η_c , brings the system to a truly first order transition [6].

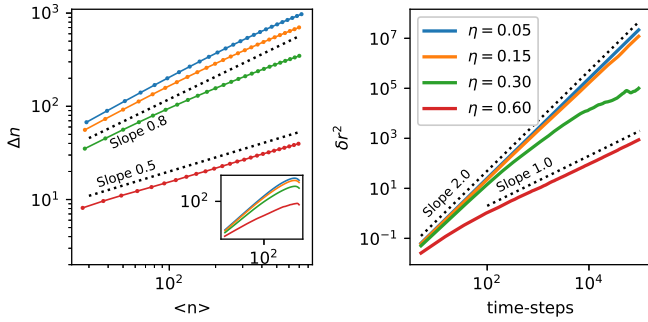


Figure 2: Giant number fluctuations for the VM (left) and mean square displacement (right) with dotted lines indicating critical slopes for the classic VM with $N = 10^4$, $\rho = 1.0$, $\Delta x = 0.03$ and various η values. Inset: Plots of GNFs for the whole range of $\langle n \rangle$ values, which shows the existence of finite size effects for large values of $\langle n \rangle$.

While the physics of this banded VM are correct, it is not valid for our purpose of modelling real animal behaviour because these bands rely on the PBCs in order to close the structure. In our study, PBCs are just a tool for the simulation to reduce the finite size effects and they shouldn't play a role on simulation results, so we won't consider that type of dynamics, in fact, we will avoid them.

This homogeneous phase where the original VM was created (without bands) is also called the Toner&Tu regime because of their work [7] where John Toner and Yuhai Tu used the main feature of this regime, i.e. statistically homogeneous density field on a large scale, as the root to their celebrated analytic hydrodynamic approach.

A very interesting observable in Vicsek-like models is the behaviour of number fluctuations. Consider a local sub-system containing on average number $\langle n \rangle$ of particles. In the dynamics were uncorrelated, fluctuations of $n(t)$, the instantaneous number of particles in the box, would be characterized by the fact that $\Delta n \equiv \langle (n(t) - \langle n \rangle)^2 \rangle^{1/2}$, the root mean square of the fluctuations, scales like $\Delta n \sim \langle n \rangle^\alpha$ with $\alpha = 0.5$ due to central limit theorem for random or equilibrium systems. Instead, here, we observe $\alpha > 1/2$ and the so-called *giant number fluctuations* (GNF) [8].

This has been measured in Figure 2 (left plot) and anomalously large fluctuations in number density have been proven in the VM. For high noise values, SPPs behave like non-correlated random walkers and we get the expected $\alpha = 0.5$ but, as η decreases, the system tends to the ordered Toner&Tu phase and fluctuations tend to grow with $\alpha = 0.8$ following the prediction from [7].

Another interesting property is the mean square displacement δr^2 which is depicted on the right-hand side of Figure 2. The phase transition here appears as a transition to $\delta r^2 \sim t^1$ for high η presenting Brownian random walkers diffusion to $\delta r^2 \sim t^2$ for low η presenting ballistic-like motion with particles moving along a stable straight line.

Global ordering (quantified by a high φ) is a collective phenomena which emerges because information about particles direction is transmitted throughout the entire group reaching a consensus even with a non zero noise amplitude. This consensus is reached, both in the VM and in our both proposed models, by an equally shared decision process, i.e. in the absence of hierarchy, leadership or any other explicit way of organization. While bigger mammals can present advanced social structures [1], fishes, as well as many insects and birds, live in groups in which members are considered to be identical (from the viewpoint of collective motion), unable to recognize each other on an individual level [1]. In these species, equally shared decision processes tend to be more beneficial primarily because they tend to produce less extreme decisions [9]. Moreover, this consensus has to be achieved via local interactions. The way these interactions work and their local effect on particle dynamics will define completely the collective behaviour.

The VM can be related easily to the ferromagnetic XY model. Both have that same degree of freedom (a spin defined with its orientation θ_i) and an equivalent interaction (alignment with local neighbourhood). Both models fuse when $\Delta x \rightarrow 0$ for the VM (static particles) resulting a fixed interaction topology. Also, when $\Delta x \rightarrow \infty$, both models may become equal in a mean-field approximation. The order parameter in the mean-field regime for the VM (for $N \rightarrow \infty$) can be proven to be $\varphi = \text{sinc}(\pi\eta)$ and the characteristic phase transition disappears. Since the XY model does not exhibit a long-range ordered phase at temperatures $T > 0$ (due to spin wave fluctuations, it only presents *quasi long range order*), the truly long-range ordered state observed in VM seems very surprising [7] and it is due to its out-of-equilibrium nature.

Furthermore, in the continuous limit of the VM (where the relaxation time for particles to change their direction to the local average direction is not zero), it can be shown that the system's spontaneous ordering behaviour has, essentially, the same type of bifurcations as the well known Kuramoto model for stochastic synchronization of oscillators. Both models show a very similar dynamic equation that becomes equal in the mean-field approximation [10].

Therefore, what makes the VM an original model is not the emerging alignment but the implications it has on the dynamics of these self-propelled particles and their interaction topology. As shown in Toner&Tu non-equilibrium continuum dynamical model [7], which describes a continuum hydrodynamic VM, what makes the VM different from other synchronization models is its particle diffusion. This keeps local interactions changing through time propagating orientational information in a super-diffusive way and brings a very dynamic interaction topology causing the non-trivial long-range order in two dimensions.

With that information in mind, now we focus our attention to the role played by individual dynamics and its response to the particle's environment while we keep using the classic VM alignment rule. In our first model, we

deep into the subtle individual changes that can have a relevant effect on the collective behaviours without leaving the Vicsek-like models philosophy.

III. A VICSEK-LIKE MODEL WITH LÉVY FLIGHTS

A. Inspiration

In H. Murakami *et al.* [3] researchers find a super-diffusive behavior on schools of ayus (*Plecoglossus altivelis*) in which fish positions (relative to the center of mass of the school) are neither fixed in time nor Brownian but display a Lévy walk pattern facilitating dynamic collective motion and information transfer throughout the group. This Lévy walk appears while the distribution function of flight distances are power-law distributed. As [11] indicates, Lévy behaviour has been found in a wide variety of species and, furthermore, it seems to be a fundamental conduct in living beings.

From those observations arises the idea to add a Lévy behaviour on VM movements and expect the system to improve communication and exhibit higher polarization for any η compared to the standard VM.

B. Model building and computational details

While in the VM (equations 1) the particles always move a fixed and constant Δx , in this new model every particle i at time t will take a uncorrelated random flight distance from a power-law distribution (in order to have a Lévy behaviour). And, in order to compare it with the classic VM, that power law distribution will be averaged to desired input parameter $\langle \Delta x \rangle$. Particle's flight distances will be random but they will have the same average displacement as their counterpart on the VM.

So, we have a power-law distribution with characteristic parameter α and, in order to have a well behaved distribution (with existing mean for $\alpha < 2$), we will set a minimum and maximum value. The power-law distribution is build as indicated below:

$$P(x) = \frac{1-\alpha}{x_{max}^{1-\alpha} - x_{min}^{1-\alpha}} x^{-\alpha} \quad \text{for } x \in [x_{min}, x_{max}] \quad (3)$$

Setting the mean of the distribution equal to one and its positive threshold to $x_{max} = 200$ (arbitrary value meaning that fishes cannot perform a flight 200 larger than the mean flight), we will have

$$\langle x \rangle = 1 = \frac{1-\alpha}{2-\alpha} \frac{x_{max}^{2-\alpha} - x_{min}^{2-\alpha}}{x_{max}^{1-\alpha} - x_{min}^{1-\alpha}} \quad (4)$$

Equation 4 cannot be solved analytically to find x_{min} but it can be solved numerically.

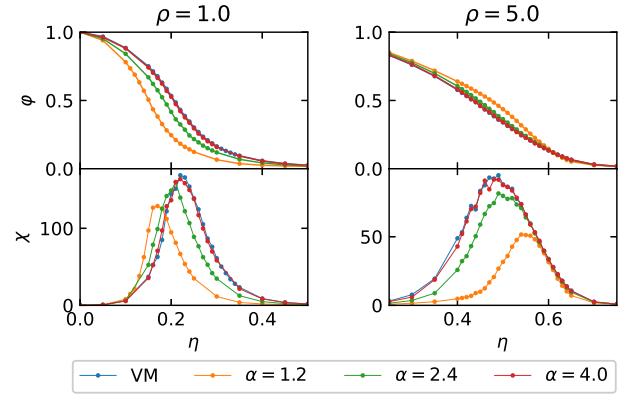


Figure 3: Polar order and its susceptibility for classic VM and our Lévy variation with $\alpha = 1.2, 2.4, 4.0$. $N = 10^4$, $\langle \Delta x \rangle = 0.03$ ($\Delta x = 0.03$ for VM), at least $3 \cdot 10^6$ time-steps and two different densities (**Left:** $\rho = 1.0$ | **Right:** $\rho = 5.0$)

Computing the cumulative distribution function $F(x)$ we can get the random value x as a function of a simpler uniform distribution $U \in [0, 1]$

$$F(x) = \int_{x_{min}}^x P(x') dx' = \frac{x^{1-\alpha} - x_{min}^{1-\alpha}}{x_{max}^{1-\alpha} - x_{min}^{1-\alpha}} \equiv U \quad (5)$$

$$x = [U (x_{max}^{1-\alpha} - x_{min}^{1-\alpha}) + x_{min}^{1-\alpha}]^{1/(1-\alpha)} \quad (6)$$

Now we have the unit-averaged distribution ready to fit in the simulation program with α exponent. If we want the distribution to be $\langle \Delta x \rangle$ -averaged we will have to multiply equation (6) by $\langle \Delta x \rangle$.

Our input parameters are the VM ones (N , η , ρ and Δx) but changing the flight distance parameter Δx for the the mean flight distance $\langle \Delta x \rangle$ and the distribution parameter α .

C. Results and discussion

Four high α values, our results show a tendency of this Lévy flights modes to reproduce the standard VM result for the group polarization. This is because, as the exponent α gets higher, the flights distribution around $\langle \Delta x \rangle$ gets sharper on the VM Δx . On the other hand, as α decreases and the distribution spreads out and starts taking a wide variety of values, the Lévy effect starts being noticeable. For $N = 10^4$ and $\rho = 1.0$, the polarization φ decreases for low α values (with greater Lévy effect) with respect to the standard VM counterpart, and so does the critical noise amplitude η_c (see Figure 3 left-hand side). This, in principle, disagrees with reported experimental data [3]. This "moderate" density scenario ($\rho = 1.0$) allows the formation of segregated noise-resistant clusters (flocks) where particles have a high number of neighbours closer than R_0 so that the external noise becomes effectively diminished in every time step. When applying the

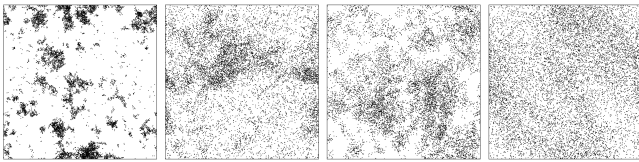


Figure 4: Screenshots of two different configurations for VM and Lévy flights model. All of them have $N = 10^4$ and $\langle \Delta x \rangle = 0.03$ ($\Delta x = 0.03$ for VM). **First:** VM with $\rho = 1.0$. **Second:** Lévy model with $\rho = 1.0$ and $\alpha = 1.2$. **Third:** VM with $\rho = 5.0$. **Fourth:** Lévy model with $\rho = 5.0$ and $\alpha = 1.2$

Lévy behaviour to SPPs, clusters melt and particles are no longer able to maintain these effectively high density groups. In the Lévy state, clusters are still present but they are much more diluted and, therefore, they lose the ability to counteract the disordering effect of noise (see the first pair of snapshots in Figure 4).

In our experimental inspiration [3], fishes never escape the flock because of their instinct to remain cohesive. In Vicsek-like models we don't use any attractive interaction so, in order to see the real effect of Lévy flights inside a stable flock, we will have to increase the density to prevent the flock diffusion.

An alternative to the density constrain could be adding new interactions to the model. There are usually attractive interactions at long enough distances in more realistic and detailed flocking simulations [4]. There, power-law flights could be applied and information would spread out through the flock without weakening it because of the attraction forces.

Here we enhance the density and set $\rho = 5.0$. Doing so, we move closer to the cluster density we observe in the standard VM simulations. Then, we check the effect of Lévy flights inside a flock and the results appear on Figure 3 (right side). Now things are different. While for high α we continue seeing results very similar to the standard VM, for low α the global order of the flock increases for any η , and so does η_c , in agreement with [3]. Here, information is spread out via power-law flights without the inconvenience of breaking the flock (see Figure 4 3rd and 4th snapshots), evidencing that a Lévy behaviour is beneficial for the orientational decision process. Long flights intensify the already high information diffusion of VM with a more complex and connected interaction network. SPPs visit a larger number of neighbours than in the VM while averaging orientations and this process enhances the global order of the flock.

IV. A MODEL WITH BURST-AND-COAST DYNAMICS AND SPEED IMITATION

A. Inspiration

The advances in image and tracking technology in real observations have made possible to obtain high preci-

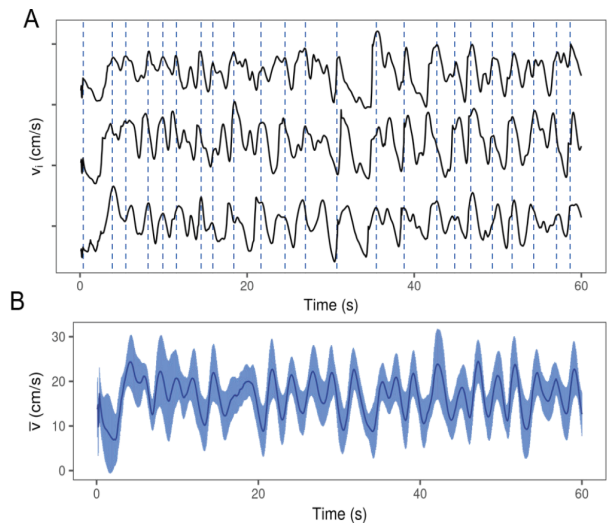


Figure 5: Experimental results from [5]. **A:** Time series of individual speeds (v_i) for three fish in a 60 seconds time lapse. Dotted vertical lines mark local maximums of upper individual. **B:** Fish mean speed (\bar{v}) and standard deviation for same time range as in A.

sion data of animals on the move [1]. Experimental data shows fine details about flocking dynamics on fishes that cannot be modelled with our previous model which studies coarse-grain mechanisms neglecting more complex behaviours at the level of individual fish.

A wide variety of fish species do not move with constant velocity nor random power-law flights but with more complex burst-and-coast dynamics [4]. These are characterized by sequences of sudden increase in speed (*kicks*) followed by a mostly passive gliding period. This coast period has been observed to describe an exponential decay of speed produced by the speed-proportional viscous water drag [4].

Burst-and-coast behaviour has also been seen by our research group in experimental observations of Black neon tetra (*Hyphessobrycon herbertaxelrodi*; one of the most popular ornamental fish species with length of 2.5 cm [5]) swimming freely in a $100 \times 93 \times 96$ cm tank in groups of 40. In these observations, fish individual trajectories and orientations in time are obtained through video recording and tracking software. Resulting data reveals oscillatory patterns in time consistent with the burst-and-coast dynamics presented on [4]. Furthermore, the group average speed (\bar{v}) has been observed to oscillate as well, indicating a synchronized collective swimming speed with direct implication on collective motion [5]. These phenomena can be seen in Figure 5 where three random particle's speeds are plotted (upper plot) and burst-and-coast behaviour is proven. In addition, on the bottom plot, synchronized speed oscillations are represented together with the standard deviation.

An interesting experimental observation of our research group is that there exists a positive correlation between group's mean swimming speed and its polarization

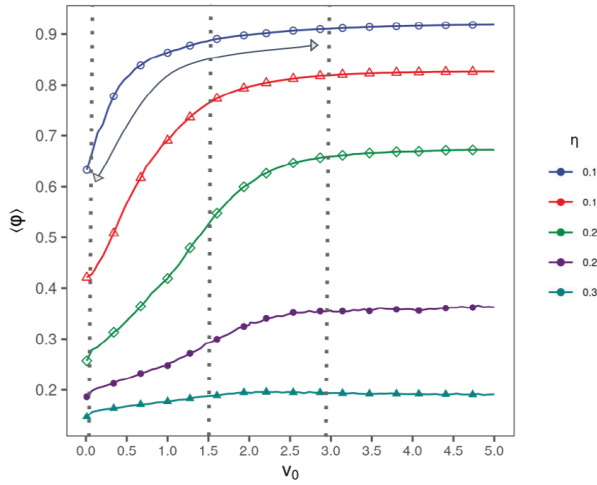


Figure 6: Results extracted from [5]. Average polarization as a function of the constant particle's speed v_0 ($v_0 \equiv \Delta x$) for different noise values in simulations of the standard VM with $N = 100$ and $\rho = 0.05$.

[5] (\bar{v} - φ correlation). In [4], modelling in detail Rummy-nose tetra (*Hemigrammus rhodostomus*), they also concluded that \bar{v} acted as a modulator on the strength of attraction and alignment interactions.

With all these experimental data in mind, scientists have worked on understanding and modelling the individual logic and interactions to reproduce this phenomenon. While in [4], authors have modelled the behaviour of groups of two fishes via highly parametrized and complex interactions describing burst-and-coast dynamics with group cohesion, a model explicitly coupling particle's speed and local polarization φ_i has also been studied to reproduce the existing correlation by explicitly introducing a direct relation of the form $v_i \sim [\varphi_i]^\alpha$ [12]. In our group [5], J. Múgica, R. Pastor-Satorras and M.C. Miguel wondered if the \bar{v} - φ correlation phenomena was achievable even in a simpler modification of the VM where SPP's exhibit a periodic speed in time.

The standard VM also exhibits a speed-driven phase transition [5] with high φ values for high enough velocities \bar{v} and vice-versa. This can be seen in Figure 6 where the simple VM has been numerically simulated around this transition range. In some way, increasing the \bar{v} is equivalent to decreasing the effect of the noise in fish matching orientations [5]. Just like flocking behaviour emerges naturally, this intrinsic phase transition in VM could be used to naturally reproduce the experimental \bar{v} - φ correlation without any other explicit constraint between particle speed and local polarization.

The authors of Ref. [5], in a low density environment mimicking real experiments ($\rho = 0.05$), take the VM with SPP's speed changing periodically with triangular oscillations. An *a priori* synchronized speed is set such that all particles perform their speed oscillations in phase. By doing so, the system is continuously forced to move on the \bar{v} -driven transition visiting both ordered and disordered

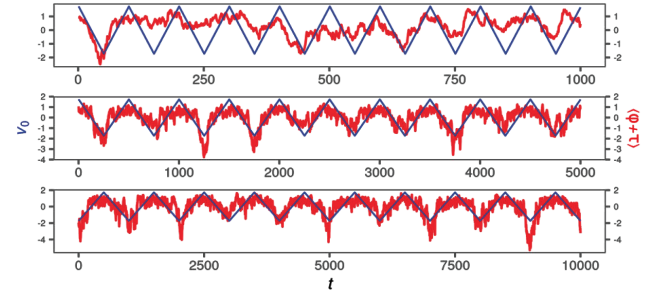


Figure 7: Results extracted from [5]. Time overlap between φ and triangular speed signals with $v_{\text{initial}} = 1.5$, $A = 1.49$, $N = 100$ and periods $T = 100, 500, 1000$. Fifty oscillation cycles are shown for each value of T .

phases. The results agree with experimental data and a positive \bar{v} - φ correlation is found (see Figure 7 where the triangular speed is plot overlapping with the polarization φ obtained for three different oscillating periods). For large enough oscillating periods, polarization indeed follows the mean speed \bar{v} dynamics with some extra fluctuations, so that correlation occurs.

With this last piece of evidence and the above experimental observations, we want to find a stochastic way to achieve collective speed changes without having to impose a synchronized speed *a priori*. Moreover, one would like to find these, more natural, speed dynamics to preserve \bar{v} - φ correlations and burst-and-coast dynamics in simulations of a Vicsek model variation, which gets closer to experimental results.

B. Model building

Starting from the standard VM classic rules, we propose to include three new mechanisms.

First, every SPP will have difficulties to move on the viscous medium (i.e., water) so that a force $F_i \propto v_i$ will be applied to it. If nothing else happens to the particle, the force will slow down particle's speed in every time-step following an exponential decay (the coast part of the *burst-and-coast* dynamics observed in fish schools [4]).

Second, at every time-step, in addition to the alignment rule, every particle will adopt the maximum value between its neighbourhood average speed and its own velocity. By implementing this imitation mechanism, a SPP will be able to make a "kick" and adapt its own velocity to that of its surroundings if necessary.

And third, during the simulation, a fixed Δv burst can randomly be added to a random SPP following a Poisson process with a uniform distribution between particles. This mechanism is consistent with the behavior observed experimentally in fish schools and, together with the second one, will enable to account for the burst part of the *burst-and-coast* dynamics observed in fish schools [4]).

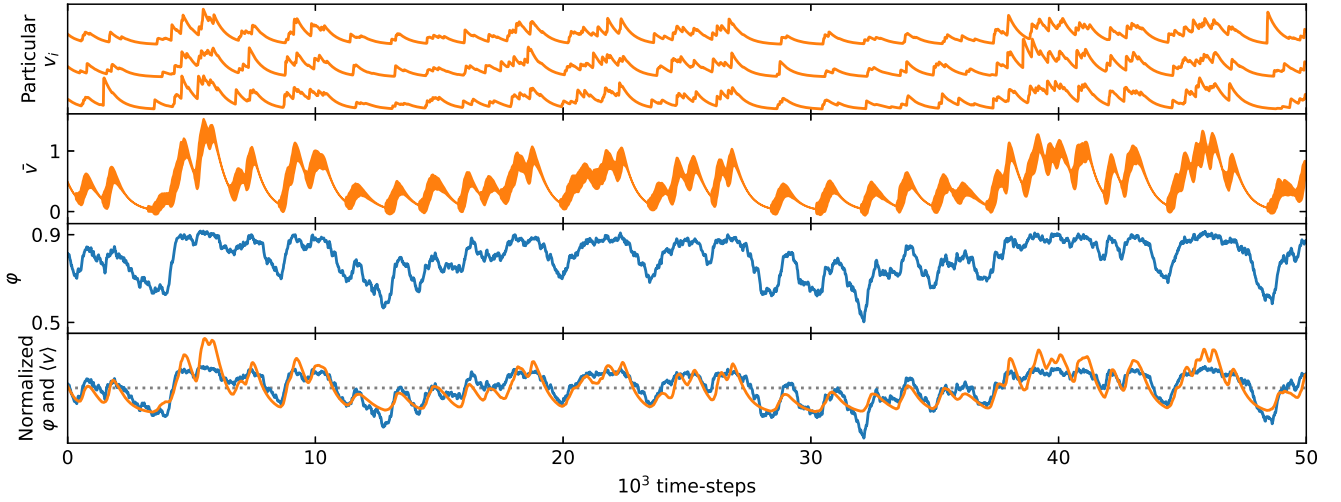


Figure 8: Temporal evolution of: **First plot**, the speed of three random SPPs in our simulations. **Second plot**, the average speed of all SPPs with its standard deviation represented in the line width. **Third plot**, group polarization. **Fourth plot**, a normalized superposition of the mean speed (orange line) and polarization (blue line). Input parameters $N = 10^3$, $\rho = 0.05$, $\eta = 0.06$, $\Delta v = 1.5$ (configuration *A* from Table I). Resulting observables $\tau = 149$, $NCC = 0.77$, $\langle \bar{v} \rangle = 0.53$ and $\langle \varphi \rangle = 0.81$. Data has been binned every 16 points in order to reduce statistical noise and improve visualization.

C. Computational details

The latter idea, consisting on Poisson speed bursts, is coded using an internal system timer. The simulation starts with timer equal to 0 and a Poisson burst occur. Knowing that bursts occur randomly with a characteristic time T , a Δt ($P(\Delta t) \sim e^{-\Delta t N/T}$) is summed to the timer and our modified VM is applied to evolve the system. In every Vicsek time-step, the timer decreases by a unit of time and it keeps going until the timer gets a negative value when another random burst occurs and the timer increases again.

In this new model, the mean flight parameter $\langle \Delta x \rangle$ disappears and 3 supplementary control parameters come into play (in addition to the remaining ones from VM). So we will have the following input parameters:

- the number of particles N ,
- the system density ρ ,
- the noise amplitude η ,
- the random burst amplitude Δv ,
- the characteristic time between consecutive random bursts T , and
- the strength of the friction force F_i .

Let us set the frictional force so that it causes a decrease on every SPP's speed of a 0.2% every time-step (a simulation time-step has always a time increment of one). Doing so, the temporal scale of the simulations is set. Also, from [5] we know that too fast \bar{v} dynamics

does not produce the corresponding φ correlation (see Figure 7 for a comparison of the influence of different oscillating periods). Dynamics with characteristic times about 500-1000 time-steps are the ones large enough to produce changes on global order. With that in mind, the characteristic time between random bursts is also set at $T = 500$ willing to see close cumulative bursts reaching high values of \bar{v} and not many $\bar{v} \approx 0$ situations. The number of control parameters has been decreased to only the firsts 4 (the same number as in the classic VM).

In order to check the \bar{v} - φ relation, a normalized cross-correlation (NCC) will be used. The NCC between two temporal vectors a_i and b_i will be defined as

$$NCC_{a,b} \equiv \frac{\sum_i (a_i - \bar{a})(b_i - \bar{b})}{\sqrt{\sum_i (a_i - \bar{a})^2 \sum_i (b_i - \bar{b})^2}} \quad -1 \leq NCC \leq 1 \quad (7)$$

where \bar{a} indicates the mean value of array a . From now on, NCC will represent the normalized cross-correlation between \bar{v} and φ .

D. Results and discussion

The first achievement of this model is the observation of a coherent dynamic group speed. The asymmetric speed interaction, using individual bursts for particles to get to their local average speed when necessary, brings a fast consensus throughout all the group in a collective swimming speed. This can be checked in Figure 8 (first two plots) where the particular speed v_i of three random particles are shown together with the group's mean speed

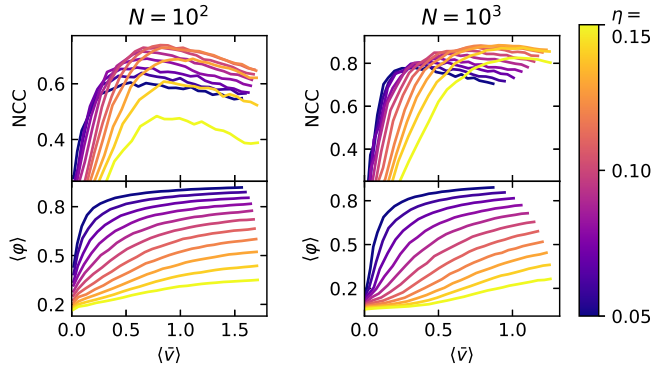


Figure 9: Normalized cross-correlation (top) and the average polarization (bottom) for $N = 100$ (left) and $N = 1000$ (right) varying the Δv parameter from 0 to 2.5 (which has an implicit relation with the mean group speed $\langle \bar{v} \rangle$) for 11 different values of η (represented with a color map).

\bar{v} and its standard deviation (s.d.) (qualitative comparison with Figure 5). With a reasonable s.d. (s.d. much smaller than fluctuations of the mean value), also present in experiments, an oscillating group speed appears as a stochastic phenomenon resembling burst-and-coast dynamics. SPPs only accelerate at some instants while, most of the time, they simply glide passively.

Before looking into the \bar{v} - φ correlations, some data corrections have to be done. A time lag τ has been measured between both observables in every simulation (just like in real experiments [5]). There exists a small relaxation time for parameter φ in order to get adapted to the current value of \bar{v} . Maximizing the correlation $NCC(\tau)$, where the temporal array φ_i is shifted by τ time-steps, we get the correlation lag. While in [5], where all particles move at the same speed, this lag exists, here it can be expected to be larger because speed kicks are not instantaneous. As the system grows, a larger number of particles have to communicate with each other in order to reach a consensus with a collective burst. This time has to be added to the intrinsic \bar{v} - φ lag. Once this time lag is "fixed" in all simulations with a φ_i shift, NCC increase by around a 5% (see Table I for exact values). All the following results have been shifted with the above method.

With some predefined input parameters (T and F_i), NCC and temporal averaged φ ($\langle \varphi \rangle$) have been measured changing N , η and Δv for a fixed $\rho = 0.05$ (the same density as in [5]), and represented in Figure 9. The change on the input parameter Δv readily implies a change on the average speed \bar{v} and, thus, on its time average value $\langle \bar{v} \rangle$. The later variable is the most relevant one so, in Figure 9, both the NCC and the mean φ are shown as a function of $\langle \bar{v} \rangle$.

The average polarization $\langle \varphi \rangle$ grows at high speeds and low noise, as expected, knowing the existence of the phase transition. In addition, for every η , a correlation peak is found just at the critical point of the speed-driven phase transition. Figure 6 shows this phase transition for simu-

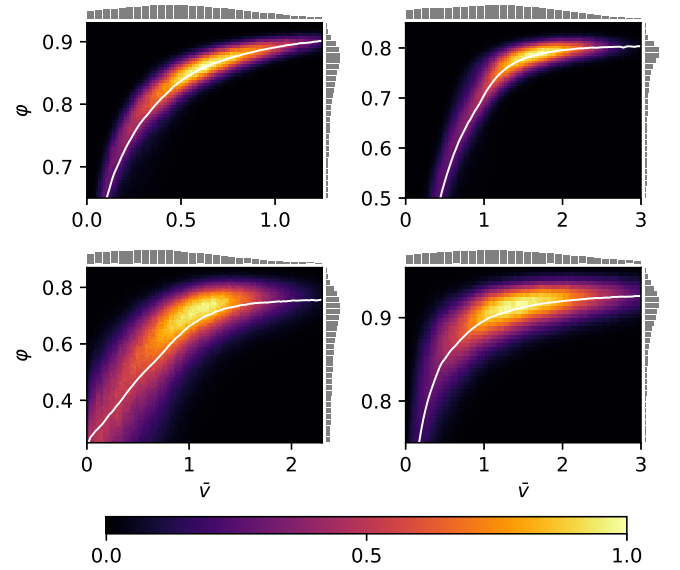


Figure 10: Normalized bidimensional histograms of φ on the y -axis and \bar{v} on the x -axis for three different system input parameters (with $\rho = 0.05$ and 10^7 VM steps of simulation) **Top left:** Configuration A from Table I. **Top right:** Configuration B. **Bottom left:** Configuration C. **Bottom right:** Configuration D. On the sides of every plot there are the one-dimensional histograms of both variables as well as the average φ for every instantaneous \bar{v} with white lines inside the images.

lations with a constant speed for all particles, and despite that's not our case, it is useful to understand our results. For high $\langle \bar{v} \rangle$, φ reaches a η -dependent threshold where fluctuations are nearly gone and, therefore, no possible \bar{v} - φ correlation can occur. On the other side, for low $\langle \bar{v} \rangle$, the dynamic range of \bar{v} is not wide enough to produce φ correlations. Just when the system's $\langle \bar{v} \rangle$ is near the critical value, any collective fluctuation in that variable can generate changes in φ increasing NCC .

The main alteration when increasing N is the (non-trivial) increase of correlation. One would expect NCC to decrease as the number of particles grows and the interaction network gets larger getting harder to reach a general consensus. While with $N = 100$ correlation reaches a maximum of $NCC = 0.74$ with $\eta = 0.11$ and $\Delta v = 1.2$, with $N = 1000$ we reach, with $\eta = 0.13$ and $\Delta v = 1.8$, an impressive maximum value of $NCC = 0.88$. These NCC peaks for $N = 1000$ occur at lower speeds compared to the ones for $N = 100$ possibly indicating the finite size dependence of this speed-driven phase transition.

Lets define now four different scenarios present in Figure 9 (A, B, C and D) and lets delve into them. The input parameters of these configuration, as well as the resulting observables, appear on Table I.

For configuration A, we can see the system temporal evolution on Figure 8. There, the \bar{v} - φ correlation becomes visible as well as the dynamic evolution of

Conf.	Input			Output					
	N	η	Δv	NCC	NCC_τ	τ	$\langle \bar{v} \rangle$ (s.d.)	$\langle \varphi \rangle$ (s.d.)	
A	10^3	0.06	1.5	0.729	0.768	149	0.53 (.31)	0.81 (.10)	
B	10^3	0.10	2.5	0.765	0.803	111	1.19 (.68)	0.66 (.18)	
C	10^2	0.11	1.2	0.700	0.731	75	0.82 (.51)	0.56 (.19)	
D	10^2	0.06	2.1	0.567	0.577	60	1.33 (.81)	0.88 (.08)	

Table I: Four different configurations to represent qualitatively the values of our model. These results correspond to a 10^7 simulation steps and show (from left to right) the correlation without and with time lag correction, the time lag for optimal NCC (measured in time-steps), the mean group speed with its standard deviation trough time and the mean polarization and its standard deviation trough time.

speed and polarization. While \bar{v} draws positive peaks, i.e. the "equilibrium" state is at low speeds and sudden bursts create positive perturbations, polarization has an opposite behaviour. φ remains mostly at high values and low values of \bar{v} make it drop to lower values. While both curves are not exactly as the experimental ones, their qualitatively behaviour is quite similar and that's a significant result. Also, configuration *D* presents very realistic observables (experimental values from [5]: $NCC_{exp} = 0.513$ (s.d. = 0.124) and $\varphi_{exp} \approx 0.88$).

For all four configuration, the bidimensional histograms of δv and ϕ are shown in Figure 10. They represent the probability to find the system any time in that \bar{v} - ϕ state. From there, correlations appear in another perspective. In all histograms, φ dependence with \bar{v} becomes more explicit. On one side, for high instantaneous \bar{v} , φ rises up to a η -dependent threshold and its fluctuations vanish with no evidence of low polarization at high speeds. On the other side, for low \bar{v} , φ drops to very low values presenting higher fluctuations.

In this Figure 10, we also show the individual histograms for both variable. In the \bar{v} histograms, a uniform distribution for most part of existing speed range is shown, from $\bar{v} = 0$ to some input-dependent value. Group speed don't have a preferred value but exhibits a broad range of them. However, φ histograms have a remarkable peak on their upper limit. It appears as a variable with a well defined central value with decreasing fluctuation (the same phenomena shown in Figure 8). This is also visible in the standard deviations of both observables in Table I where temporal fluctuations take an average value of 59.7% of the mean value for \bar{v} but only 18.9% for φ .

As a final measurement, the cumulative distribution functions of all individual speeds during the simulation for our four scenarios have been plotted in Figure 11 (left). In the right side of this Figure appears the experimental cumulative distribution function of flight distance defined as the distance travelled in a straight line (with rotations smaller than a fixed threshold). The speed in our model can be related to the flight distance in real experiments as our SPPs rotate every time step so the

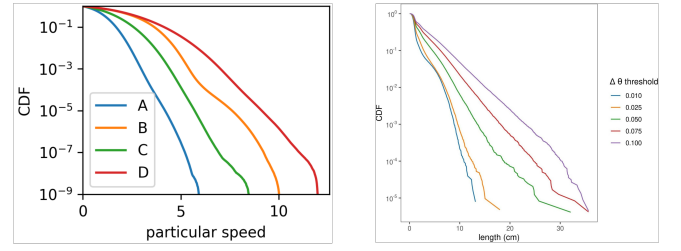


Figure 11: **Left:** Cumulative distribution function of SPPs instant speeds in the burst-and-coast model for the four configuration of table I **Right:** Cumulative distribution function of flight lengths between two consecutive reorientations from our research group experimental observations on Black neon tetra (different threshold are tested to determine a change on orientation).

distance travelled in one step is $\Delta x = \Delta t v_i = v_i$. Our observations show an exponential decay of flight lengths which appears also (at least qualitatively) in our model.

V. CONCLUSIONS

In this project the classic Vicsek model has been revisited so that its phase transition, GNF and mean square displacement have been obtained and reviewed. Moreover, inspired by published experimental data and our own group experimental observations of real fish schools, we have proposed two new models to analyze the collective motion of these animals. Although the approach in both models is very different, they share a key common factor: The Vicsek philosophy is present in both models with equally shared decision processes and the alignment law. Moreover, both models remain as simple as possible without over-parameterizing the system. This makes them more universal and useful for other types of collective motion.

In the Lévy flights model, our first model, we prove that simple changes in individual dynamics, with Lévy behaviour and power-law flight displacements, improves social connectivity of SPPs within the group. This has a biological benefit, a reinforcement of collective order in front of external perturbations. This effect is true while the group remains cohesive. For densities lower than the intrinsic VM flocking density, this power-law flights have a counterpart. The diffusion of SPP to the outside of the flock induced by their Lévy behaviour (assuming no attraction interactions to keep the flock together) is a handicap that weakens flocking structures and, thus, the collective strength that these structures bring.

Our second model, the Poisson burst-and-coast dynamics with speed imitation, reveals various non-trivial characteristics. A variable group speed is reached without being explicitly imposed. Three very natural and experimental based laws are enough to reproduce qualitatively the observed burst-and-coast dynamics on fishes and to induce a very dynamic collective movement. This

improves collective performance in nature because these synchronized burst-and-coasts may be more energy efficient than asynchronous ones by limiting water flow speed fluctuations [4]. In addition, this stochastic group speed fluctuation has been proved to reproduce our previous results in the research group [5] presenting high positive cross-correlation with global polarization. This phenomena has not been explicitly imposed but it has been accomplished using simple Vicsek-like rules.

Future advances in the area should focus in the direction of getting more and better experimental data of free animal groups. Observations and, thus, its conclusions, tend to be constrained by the laboratory limitations. One could expect the animal behaviour to be very different in open space than in an experimental building and, thus, more efforts may have to be done to delve deeper into the intriguing mechanisms of collective motion.

Acknowledgments

I would like to thank deeply my advisor, M. Carmen Miguel, for her constant dedication, help, inspiration and generosity. I would also like to thank UNIVERSITAT DE BARCELONA and UB INSTITUTE OF COMPLEX SYSTEMS (UBICS) for letting me take this Final Master Project with them with a collaboration scholarship of 25 hours per week.

COVID-19 pandemic has complicated the development of this project with social distancing affecting the expected communication within the workgroup. For that, I appreciate so much the effort of all the academic community for keep working and going ahead. In these difficult times I have to deeply thank Irina for supporting me at home every difficult day of this confined project.

-
- [1] Tamás Vicsek and Anna Zafeiris. Collective motion. *Physics Reports*, 517(3-4):71–140, Aug 2012.
 - [2] Tamás Vicsek, András Czirók, Eshel Ben-Jacob, Inon Cohen, and Ofer Shochet. Novel type of phase transition in a system of self-driven particles. *Phys. Rev. Lett.*, 75:1226–1229, Aug 1995.
 - [3] Hisashi Murakami, Takayuki Niizato, Takenori Tomaru, Yuta Nishiyama, and Yukio-Pegio Gunji. Inherent noise appears as a lévy walk in fish schools. *Scientific reports*, 5:10605, 06 2015.
 - [4] Daniel Calovi, Alexandra Litchinko, Valentin Lecheval, Ugo Lopez, Alfonso Escudero, Hugues Chaté, Clément Sire, and Guy Theraulaz. Disentangling and modeling interactions in fish with burst-and-coast swimming reveal distinct alignment and attraction behaviors. *PLOS Computational Biology*, 14:e1005933, 01 2018.
 - [5] Julia Múgica, Romualdo Pastor-Satorras, and M. Carmen Miguel. Collective ordering dependence on swimming speed: Experimental and theoretical comparisons. *Preprint*, 2020.
 - [6] Hugues Chaté, Francesco Ginelli, Guillaume Grégoire, and Franck Raynaud. Collective motion of self-propelled particles interacting without cohesion. *Physical Review E*, 77(4), Apr 2008.
 - [7] John Toner and Yuhai Tu. Long-range order in a two-dimensional dynamical XY model: How birds fly together. *Phys. Rev. Lett.*, 75:4326–4329, Dec 1995.
 - [8] Hugues Chaté, Francesco Ginelli, Guillaume Grégoire, Fernando Peruani, and Franck Raynaud. Modeling collective motion: Variations on the vicsek model. *Eur. Phys. J. B*, 64:451–456, 08 2008.
 - [9] Larissa Conradt and Timothy Roper. Consensus decision making in animals. *Trends in ecology & evolution*, 20:449–56, 09 2005.
 - [10] A.A. Chepizhko and V.L. Kulinskii. On the relation between vicsek and kuramoto models of spontaneous synchronization. *Physica A: Statistical Mechanics and its Applications*, 389(23):5347–5352, 2010.
 - [11] V. Zaburdaev, S. Denisov, and J. Klafter. Lévy walks. *Reviews of Modern Physics*, 87(2):483–530, Jun 2015.
 - [12] Shradha Mishra, Kolbjørn Tunstrøm, Iain D. Couzin, and Cristián Huepe. Collective dynamics of self-propelled particles with variable speed. *Phys. Rev. E*, 86:011901, Jul 2012.
 - [13] Jordi Torrents Monegal. Simulation program for vicsek model and our variations. Available at https://github.com/xurxo12/TFM_program.
 - [14] Collaboratory for advanced Computing and Simulations (University of Southern California). Linked-list cell molecular dynamics. Available at <http://cacs.usc.edu/education/cs596/01-1LinkedListCell.pdf>.

VI. COMPUTATIONAL APPROACH

100% of the used code in this project has been written by the author. It is a sequential modular program in Fortran ready to use in Linux (but easily adaptable to Windows or iOS) and with an extensive input file to be able to choose any configuration or model as desired. The hole program is in a GitHub repository [here](#) [13] ready to use together with some Python scripts to plot the results.

To simulate up to 10^4 particles in a reasonable computing time, the program has been optimized with primarily two main algorithms. The first one is the *linked lists* data algorithm to find particle's positions rapidly. It is fully computational, meaning that it has no effect on numerical results. The second one is the *complete cell* interaction in which we achieve to remove any distance computation. It implies numerical discrepancies in a detailed scale but it doesn't have an affect on system's global behaviour (at least, for large enough systems).

The naive double-loop implementation to compute pair interactions scales as $\mathcal{O}(N^2)$ with N particles and most of the distance computations are not relevant if a threshold is used in the simulations (as we do in Vicsek-like models). Thus, another algorithm should be used to compute distances in a more efficient way. Gridding the simulation space into unitary cells and using *Linked lists* data structure, we are able to build two one-dimensional arrays of length N clustering all particles inside every cell they belong to. Doing so, we will have the list of all particles inside any cell in a very accessible and fast way. As this is not a relevant topic for this paper, a brief explanation of *Linked lists* algorithm can be found on this UNIVERSITY OF SOUTHERN CALIFORNIA little manual [14]. The main advantage of this ceiling lists method is the computational lightness of its building and use.

The *complete cell* interaction consists on modifying the pair interaction term of VM equations $\langle \theta_j^t \rangle_{j \in R_0}$ (Equation 1) in which the pair i - j interacts only if its distance is closer than $R_0 \equiv 1$. With all particles listed on their unit-area cell (using the previous *Linked lists* method), the idea is to expand the interaction area to all particles of the 9 neighbours cells (including their own cell). Doing so, no distance computation is required and the simulation speeds up. Nevertheless, interaction area has changed and that has a huge effect on system's behaviour, simulation program will have to work on a set of modified internal control parameters (η' , $\Delta x'$ and ρ') to counteract this implementation.

Modified density ρ' can be computed relating the average number of particles on the initial interaction area, which is the area of a radius 1 circle, with the new mean number of particles in the new interaction area of 9 unit-size cells. Setting them to be equal we will have $\pi\rho = 9\rho'$. For $\Delta x'$ we match the ratio between the mean flight and the linear size (the radius of the equivalent circle with the same area) of the interaction zone ($\Delta x/1 = \Delta x'/\sqrt{9/\pi}$). Finally, as this is a spatial transformation, no modifications on η is needed so internal control parameters now become

$$\eta' = \eta \quad ; \quad \Delta x' = \frac{3}{\sqrt{\pi}}\Delta x \quad ; \quad \rho' = \frac{\pi}{9}\rho \quad (8)$$

Measuring the CPU time for the three different approaches with different number of particles on the VM, we get Figure 12. Fits show a dependence of time as $t_{\text{CPU}} \sim N^\delta$ for the three algorithms. The naive double loop (simplest and most expensive distance computation) has $\delta \approx 1.85$, using linked lists to store particle position information and checking distances only with neighbours cells particles has $\delta \approx 1.32$ and the complete cell interaction where no distance is computed gets a $\delta \approx 1.05$. The improvement is huge and it bring the opportunity to reach 10^4 particles on extensive simulations without having to paralyze the program.

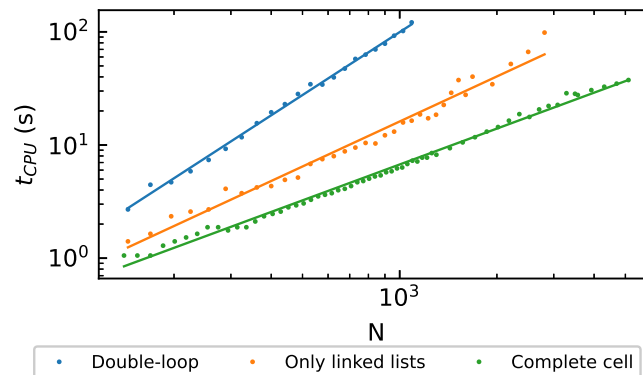


Figure 12: Computational time for three different interaction algorithms as a function of N (points) with power-law adjusts (lines) (computing VM).